13. Lamberts SWJ, Bakker WH, Reubi J-C, Krenning EP. Somatostatin-receptor imaging in the localization of endocrine tumors. *N Engl J Med* 1990;323:1246–1249.
14. Redding TW, Schally AV. Inhibition of growth of pancreatic carcinomas in animal models by analogs of hypothalamic hormones. *Proc Natl Acad Sci* 1984;81:248–252.
15. Reubi J-C. A somatostatin analog inhibits chondrosarcoma and insulinoma tumor growth. *Acta Endocrinol* 1985;109:108–114.
16. Liebow C, Reilly C, Serrano M, Schally V. Somatostatin analogs inhibit growth of pancreatic cancer by stimulating tyrosin phosphatase. *Proc Natl Acad Sci* 1989;86: 2003–2007.
17. Krenning EP, Kooij PPM, Bakker WH, et al. Radiotherapy with a radiolabeled somatostatin analog, [^{111}In-DTPA-d-Phe^1]-octreotide. *Ann NY Acad Sci* 1994;733: 496–506.
18. Priester WA. Pancreatic islet cell tumors in domestic animals. Data from 11 colleges of veterinary medicine in the United States and Canada. *J Nat Cancer Inst* 1974;53: 227–229.
19. Caywood DD, Klausner JS, O'Leary TP, et al. Pancreatic insulin-secreting neoplasms: clinical, diagnostic and prognostic features. *J Am Anim Hosp Assoc* 1988;24:577–584.
20. Leifer CE, Peterson ME, Matus RE. Insulin-secreting tumor: diagnosis and medical and surgical management in 55 dogs. *J Am Vet Med Assoc* 1986;188:60–64.
21. Dunn JK, Heath MF, Herrtage ME, Jackson KF, Walker, MJ. Diagnosis of insulinomas in the dog: a study of 11 cases. *J Small Animal Pract* 1992;33:514–520.
22. Trinder P. Determination of glucose in blood using glucose oxidase with an alternative oxygen acceptor. *Ann Clin Biochem* 1969;6:24–27.
23. Reubi J-C. New specific radioligand for one subpopulation of brain somatostatin receptors. *Life Sci* 1985;36:1829–1836.
24. Hofland LJ, van Koetsveld PM, Wouters N, Waaijers M, Reubi J-C, Lamberts SWJ. Dissociation of antiproliferative and antihormonal effects of the somatostatin analog octreotide on 7315b pituitary tumor cells. *Endocrinology* 1992;131:571–577.
25. Scatchard G. The attractions of proteins for small molecules and ions. *Ann NY Acad Sci* 1949;51:660–672.
26. Evans HE. The digestive apparatus and abdomen: the pancreas. In: Evans HE, ed. *Miller's anatomy of the dog*, 3rd ed. Philadelphia: W.B. Saunders Co.; 1993:458–460.
27. Leifer CE, Peterson ME, Matus RE, Patnaik AK. Hypoglycemia associated with nonislet cell tumor in 13 dogs. *J Am Vet Med Assoc* 1985;186:53–55.
28. Dunn JK, Bostock DE, Herrtage ME, Jackson KF, Walker HJ. Insulin-secreting tumors of the canine pancreas: clinical and pathological features of 11 cases. *J Small Animal Pract* 1992;34:325–331.
29. Campbell JP, Wilson SR. Pancreatic neoplasms: how useful is evaluation with US. *Radiology* 1988;167:341–344.
30. Hall-Craggs MA, Lees WR. Fine-needle aspiration biopsy: pancreatic and biliary tumors. *Am J Roentgenol* 1986;147:399–403.
31. Reichlin S, Somatostatin (second of two parts). *N Engl J Med* 1983;309:1556–1563.
32. Ur E, Bomanji J, Mather SJ, Britton KE, Wass JAH, Grossman AB, Besser GM. Localization of neuroendocrine tumors and insulinomas using radiolabeled somatostatin analogs, ^{123}I-Tyr^3-octreotide and ^{111}In-pentatreotide. *Clin Endocrinol* 1993;38: 501–506.
33. Kubota A, Yamada Y, Kagimoto S, et al. Identification of somatostatin receptor subtypes and an implication for the efficacy of somatostatin analog SMS 201–995 in treatment of human endocrine tumors. *J Clin Invest* 1994;93:1321–1325.
34. Bruns C, Weckbecker G, Raulf F, et al. Molecular pharmacology of somatostatin-receptor subtypes. *Ann NY Acad Sci* 1994;733:138–146.
35. Lamberts SWJ. Nonpituitary actions of somatostatin. A review on the therapeutic role of SMS 201–995 (sandostatin). *Acta Endocrinol* 1986;276 (suppl):41–55.

Synthesis, Biodistribution and Imaging Properties of Indium-111-DTPA-Paclitaxel in Mice Bearing Mammary Tumors

Chun Li, Dong-Fang Yu, Tomio Inoue, David J. Yang, Wayne Tansey, Chun-Wei Liu, Luka Milas, Nancy R. Hunter, E. Edmund Kim and Sidney Wallace

Division of Diagnostic Imaging and Department of Experimental Radiotherapy, The University of Texas M.D. Anderson Cancer Center, Houston, Texas

Paclitaxel, an antineoplastic agent that stabilizes microtubules and arrests cells in the G2/M cell cycle phase, has shown activity against many common cancers, including ovarian and breast tumors. In order to evaluate the potential value of radiolabeled paclitaxel as an imaging tool in tumors, we synthesized ^{111}In-DTPA-paclitaxel and investigated its biodistribution and gamma scintigraphic imaging properties. **Methods:** Mice bearing a paclitaxel-responsive mammary tumor (MCA-4) were used. DTPA-paclitaxel was labeled with ^{111}In with a radiochemical yield of 84% and radiochemical purity of 90%. Each mouse received 5 μCi of radiotracers intravenously for biodistribution studies and 100 μCi for gamma scintigraphic studies. Indium-111-DTPA was used as a control. **Results:** In tumor-bearing mice, ^{111}In-DTPA was characterized by rapid clearance from the plasma with negligible retention in the tumor, the liver and other body parts. In contrast, ^{111}In-DTPA-paclitaxel exhibited a pharmacological profile resembling that of paclitaxel. Furthermore, a significant uptake of ^{111}In-DTPA-paclitaxel was observed in the tumor. The tumor-to-muscle ratios were 2.64, 3.16 and 6.94 at 30 min, 2 hr and 24 hr, respectively, although absolute uptake in the tumor decreased from 1.95% (injected dose/g) at 30 min to 0.21% at 24 hr after injection. The tumor-to-blood ratio reached 50 at 24 hr after injection. Gamma scintigraphy and autoradiographic studies clearly showed the retention of radiolabeled paclitaxel in the tumor 24 hr after injection. **Conclusion:** These studies suggest that ^{111}In-DTPA-paclitaxel may be clinically useful in studying the uptake of paclitaxel in solid tumors.

Key Words: paclitaxel; biodistribution; gamma scintigraphy; indium-111; DTPA

J Nucl Med 1997; 38:1042–1047

Paclitaxel (Taxol) has shown a remarkable antineoplastic effect in human cancer in Phase I studies and early Phase II and III trials (*1,2*). In advanced ovarian and breast cancer patients who had received multiple prior treatment regimens, response rates of 20%–37% were observed (*2*). Significant activity also has been documented in small-cell and nonsmall-cell lung cancer, head and neck cancers and metastatic melanoma. The antitumor action of paclitaxel is due principally to inhibition of the disassembly of microtubules into tubulin (*1*). Recently, paclitaxel also was shown to be a potent antiangiogenic agent in both normal and tumor-induced angiogenesis (*3*).

The rationale for synthesizing and evaluating indium-labeled paclitaxel is as follows. First, paclitaxel is unique in its mechanism of action as an antimitotic agent and antiangiogenic agent. Given the efficacy of paclitaxel in the treatment of human cancer, the unique binding site for paclitaxel or paclitaxel analogs on the microtubules of the proliferating cells may be an attractive target for selective tumor imaging. As an antiangiogenic agent, radiolabeled paclitaxel may also be used as a tool to image tumor-induced angiogenesis. Second, the

Received Mar. 27, 1996; revision accepted Oct. 2, 1996.

For correspondence or reprints contact: Chun Li, PhD, M.D. Anderson Cancer Center, Department of Diagnostic Radiology, Box 59, 1515 Holcombe Blvd., Houston, TX 77030.

synthesis and evaluation of radiolabeled paclitaxel in animals are prerequisites to the study of its possible use for the prediction of chemotherapeutic efficacy with paclitaxel in cancer patients. Paclitaxel is extracted from the needles and bark of the Pacific yew tree. Due to the limited resources from which paclitaxel is produced, Taxol therapy is very expensive. It is reasoned that if an imaging technique can be used to predict the response of Taxol and to properly select the patients to be treated, great expense and crucial time may be saved for the patient. Our assumption is that if there is no reasonable amount of the chemotherapeutic agent deposited in the tumor, the probability of tumor response to that agent is relatively small. Third, although several studies in clinical trials have been performed to determine the pharmacological behavior of Taxol (*4*), tumor uptake of paclitaxel in patients has never been evaluated directly. Therefore, an imaging technique that allows the determination of in vivo pharmacokinetic properties of paclitaxel would be highly desirable. Indium-111 with a half-life of 67 hr is ideal for delayed imaging studies in animals.

In this study, radiolabeling of paclitaxel was performed using DTPA as a chelating agent. We investigated tissue distribution, gamma scintigraphy and autoradiographic studies of ^{111}In-DTPA-paclitaxel in tumor-bearing mice. The MCA-4 tumor was selected because the tumor model was known to respond to paclitaxel (*5*). In these studies, ^{111}In-DTPA was used as a control.

MATERIALS AND METHODS

General Chemistry

Diethylenetriaminepentaacetic acid anhydride (DTPA-A), N,N-dimethylformamide (DMF), and dimethylsulfoxide (DMSO) were obtained from Sigma (St. Louis, MO). Paclitaxel (purity > 97%) was purchased from Hande Tech (Houston, TX) or from Napro Biotherapeutics (Boulder, CO). Sodium acetate, sodium citrate was purchased from EM Science (Gibbstown, NJ). Preparative reversed-phase thin-layer chromatographic (TLC) plates (Whatman, 1000 μm layer) were obtained from Curtin Matheson Scientific, Inc. (Houston, TX). Indium-111-chloride (specific activity 416 Ci/mg) was obtained from DuPont NEN (Boston, MA). All materials were used as received.

Melting points were measured with a Mel-Temp II and left uncorrected. Ultraviolet spectra (UV) were obtained on a Beckman DU-70 spectrophotometer (Fullerton, CA). Proton nuclear magnetic resonance (^{1}H NMR) spectra were obtained by using a GE-300 MHz spectrometer. Chemical shifts are reported in ppm on the δ scale relative to TMS (DMSO-d_6). Fast atom bombardment-mass spectra (FAB-MS) were measured with a Kratos MS-50 (UK) spectrometer with nitrobenzylalcohol as a matrix. Elemental analyses were measured by Galbraith Laboratories (Knoxville, TN).

Synthesis of 7-DTPA-Paclitaxel

Diethylenetriaminepentaacetic acid anhydride (DTPA-A; 210 mg, 0.585 mmol) at 0°C was added to a solution of paclitaxel (100 mg, 0.117 mmol) in dry DMF (2.2 ml). The reaction mixture was stirred at 0°C for an additional 2 hr and then at 4°C overnight. The suspension was filtered (0.2 μm Millipore filter) to remove unreacted DTPA-A. The filtrate was poured into distilled water, stirred at 4°C for 20 min, and the precipitate collected. The crude product was purified by preparative TLC over C18 silica gel plates and developed in acetonitrile/water (1:1). Paclitaxel had an R_f value of 0.18. The band above the paclitaxel with an R_f value of 0.73 was removed by scraping and eluted with an acetonitrile/water (1:1) mixture, and the solvent was evaporated to give 15 mg of 7-DTPA-paclitaxel (yield 10.4%): mp: > 226°C dec. UV spectrum (sodium salt in water) had maximal absorption at 228 nm that is also characteristic for paclitaxel. Mass spectrum was (FAB) m/e 1229 (M+H), 1251 (M+Na), 1267 (M+K). In the ^{1}H NMR (DMSO-d_6) the resonance of NCH_2CH_2N and CH_2COOH of DTPA appeared as a complex series of signals at δ 2.71–3.03 ppm and as a multiplet at δ 3.39 ppm. The resonance of C7-H at 4.10 ppm in paclitaxel shifted to 5.32 ppm (dd), suggesting esterification at 7 position. The rest of the spectrum was consistent with the structure of paclitaxel.

Radiolabeling of DTPA-Paclitaxel with Indium-111

Into a 2-ml V-vial were added successively 40 μl 0.6 *M* sodium acetate (pH 5.3) buffer, 40 μl 0.06 *M* sodium citrate buffer (pH 5.5), 20 μl DTPA-paclitaxel solution in ethanol (2% w/v) and 20 μl $^{111}InCl_3$ solution (1.0 mCi) in a sodium acetate buffer (pH 5.5). After an incubation period of 30 min at room temperature, the labeled ^{111}In-DTPA-paclitaxel was purified by passing the mixture through a C18 Sep-Pak cartridge using saline and subsequently methanol as the eluent. Free ^{111}In-DTPA (<3%) was removed by saline, while ^{111}In-DTPA-paclitaxel was collected in the methanol solution. After methanol was evaporated under nitrogen, the residue was dissolved in 5 ml of saline and filtered through a sterile Millipore filter (0.22 μm).

HPLC (System I) was used to analyze the reaction mixture and purity of ^{111}In-DTPA-paclitaxel. The system consisted of an LDC binary pump, a 100-mm x 8.0-mm (i.d.) Waters column filled with ODS 5 μm silica gel. The column was eluted at a flow rate of 1 ml/min with a gradient mixture of water and methanol (gradient from 0% to 85% methanol over 15 min). The gradient system was monitored with a NaI crystal detector and a Spectra-Physics UV/Vis detector.

Radiolabeling of DTPA with Indium-111

Into a 2-ml V-vial were added successively 40 μl 0.6 *M* sodium acetate (pH 5.3) buffer, 40 μl 0.06 *M* sodium citrate buffer (pH 5.5), 20 μl DTPA solution in water (2% w/v) and 20 μl $^{111}InCl_3$ solution (1.0 mCi) in a sodium acetate buffer (pH 5.5). After an incubation period of 30 min at room temperature, the mixture was passed through a C18 Sep-Pak cartridge using saline as the eluent. The final volume was adjusted with saline to 5 ml. Radiochemical yield 89%.

Stability of 7-DTPA-Paclitaxel

The 7-DTPA-paclitaxel was dissolved in a phosphate buffered solution (10 m*M*, pH 7.4) (1.0 mg/ml), and the solution was incubated at 37°C. At various intervals, aliquots were drawn and analyzed by HPLC. The HPLC system (System II) consisted of a Waters 150 × 3.9 (i.d.)-mm C18 Nova-Pak column, a Perkin-Elmer isocratic LC pump, a PE Nelson 900 series interface, a Spectra-Physics UV/Vis detector and a data station. The mobile phase (methanol-0.02 *M* ammonium acetate = 3:2) was run at 2.0 ml/min with UV detection at 228 nm. The retention times of 7-DTPA-paclitaxel and taxol were 3.30 and 16.85 min, respectively. Peak areas were quantitated and compared with a standard curve to elucidate the 7-DTPA-paclitaxel concentrations.

To estimate the stability of ^{111}In-DTPA-paclitaxel, a solution of the radiotracer in saline was allowed to stand at room temperature for up to 7 days. Aliquots were drawn and analyzed by HPLC (System I) for the presence of ^{111}In-DTPA-paclitaxel. The percentages of radioactivity associated with ^{111}In-DTPA-paclitaxel peak were determined.

Cytotoxicity of 7-DTPA-Paclitaxel

B16 mouse melanoma cells and 13762 mammary breast cells (obtained from the Department of Veterinary Medicine, The University of Texas M.D. Anderson Cancer Center, Houston, TX) were used to study the cytotoxicity of 7-DTPA-paclitaxel. Cells were seeded in a 24-well plate at a concentration of 2.5 × 10^4

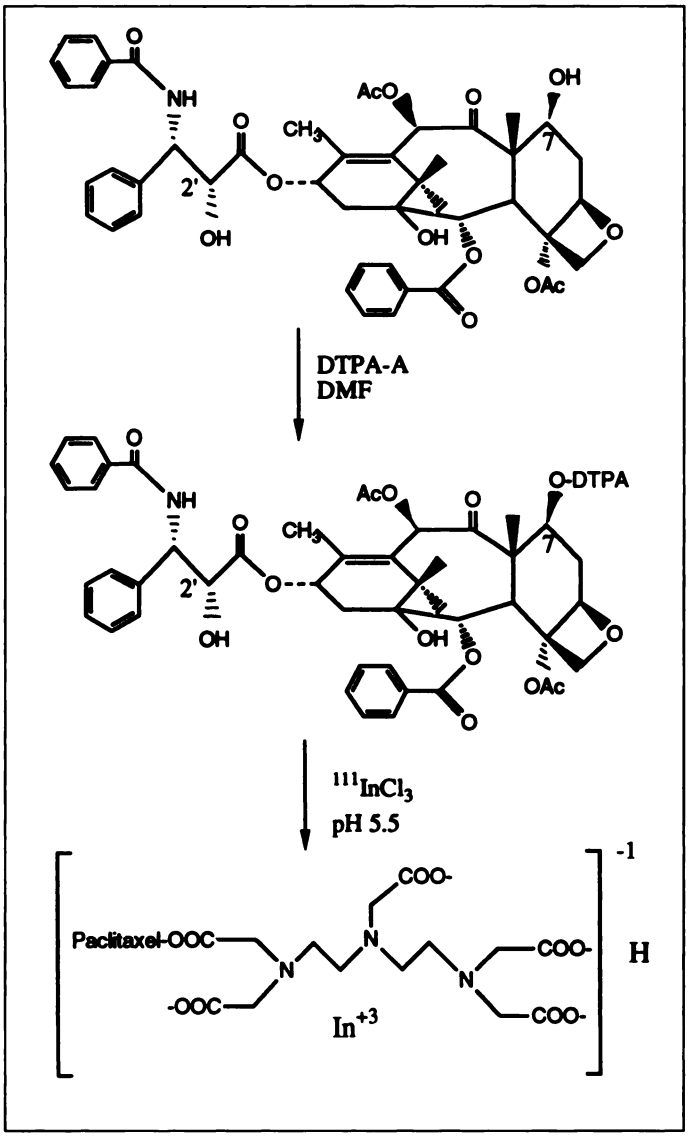

FIGURE 1. Reaction scheme for the synthesis of 7-DTPA-paclitaxel and its conjugation with ^{111}I. DTPA-A = diethylenetriaminepentaacetic acid anhydride.

cells/ml and grown in 50:50 Dulbecco's modified minimal essential medium (DME) and F12 medium containing 10% bovine calf serum at 37°C for 24 hr in a 97% humidified atmosphere of 5.5% CO_2. The medium was then replaced with fresh medium containing paclitaxel or DTPA-paclitaxel in concentrations ranging from 5×10^{-9} M to $75 \times 10-9$ M. After 40 hr, the cells were released by trypsinization and counted in a Coulter counter. DMSO was used to dissolve paclitaxel while 0.05 *M* sodium bicarbonate aqueous solution was used to dissolve DTPA-paclitaxel. The final concentrations of DMSO in the cell medium were less than 0.01%. This amount of agents did not have any effect on cell growth as determined by control experiments.

Biodistribution of Indium-111-DTPA-Paclitaxel and Indium-111-DTPA in Mice

Female C3Hf/Kam mice were inoculated with mammary carcinoma (MCA-4) in the muscles of the right thigh (5×10^5 cells). The mice (20–25 g) were bred and maintained in our specific pathogen-free mouse colony in the Department of Experimental Radiotherapy. When the tumors had grown to 10–12 mm in diameter (after approximately 3 wk), the mice were divided into groups of five. Indium-111-DTPA-paclitaxel or ^{111}In-DTPA was given to the mice through the tail vein at a dose of 5 μCi in 0.15 ml. Animals were killed at 30 min, 2 hr, 4 hr, 24 hr and 48 hr after injection. Various tissues, including tumor tissues, were collected, weighted and counted for radioactivity. The percent of the injected dose per gram of tissue weight was calculated.

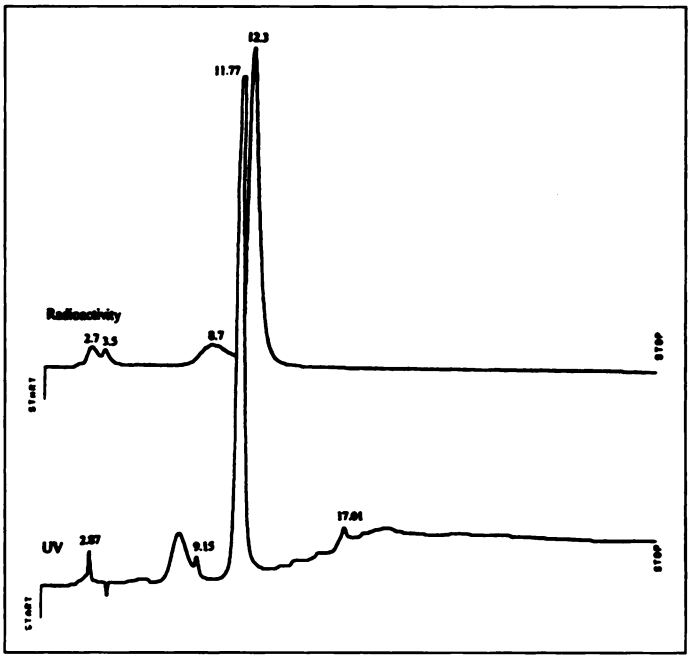

FIGURE 2. HPLC chromatograms of radiolabeled ^{111}In-DTPA-paclitaxel. The radiochromatogram of ^{111}In-DTPA-paclitaxel (retention time 12.3 min; top) correlated with its UV chromatogram (bottom). See text for HPLC conditions.

Whole-Body Scintigraphy

Six female C3Hf/Kam mice bearing MCA-4 tumor (10–12 mm in diameter) were divided into two groups (three mice per group). For Group 7, the mice were anesthetized by an intraperitoneal injection of sodium pentobarbital and were then administered ^{111}In-DTPA-paclitaxel (100 μCi, 0.6 ml) through the tail vein. A gamma camera equipped with a medium-energy collimator was positioned over the mice. A series of 5-min acquisitions was collected at 5 and 30 min and 1 , 2 , 4 and 24 hr after injection. For Group 2, the same procedures were followed except that the mice were injected with ^{111}In-DTPA as a control.

Autoradiographic Studies

After receiving ^{111}In-DTPA-paclitaxel, two female tumor-bearing C3Hf/Kam mice were killed at 2 hr after injection (100 μCi, intravenously). The body was then fixed in a carboxymethyl cellulose (4%) block. The frozen body was mounted to a cryostat (LKB 2250 cryo-microtome, Ijamsville, MD), and 100-μm coronal sections were made. The section was thawed and mounted on a slide. The slide was placed in contact with x-ray film for 48 hr.

Statistical Analysis

The significance of difference in tumor uptake between ^{111}In-DTPA-paclitaxel and ^{111}In-DTPA was analyzed by unpaired, two-tailed Student's t-test, and p was set at 0.05.

RESULTS

Synthesis and Characterization

The synthesis of DTPA-paclitaxel was performed by directly reacting DTPA anhydride with paclitaxel as shown in Figure 1. Under the reaction conditions used, both paclitaxel C-2′ and C-7 ester were obtained. C-2′ ester of DTPA was unstable in an aqueous solution. Treatment with water resulted in hydrolysis of C-2′ ester, leaving C-7 ester as one of the major products.

TABLE 1
Cytotoxicity of Paclitaxel and 7-DTPA-Paclitaxel against B16 Melanoma and 13762 Mammary Tumor Cells*

Compound	IC_{50} (nM)	
	B16	13762
Paclitaxel	15	13
7-DTPA-paclitaxel	10	17

*Data were derived from cell density-concentration curves.

Purification of 7-DTPA-paclitaxel was achieved by preparative C18 TLC. A substantial amount of paclitaxel (approximately 40%) also was recovered from the TLC plates, which was recycled. The structure of the product was identified by NMR and mass spectroscopy. The presence of metal salts (sodium, potassium) precluded obtaining an accurate elemental analysis. UV spectrum of aqueous solution of DTPA-paclitaxel sodium salt was identical to that of paclitaxel.

Conjugation of ^{111}In to 7-DTPA-paclitaxel was achieved by simply mixing DTPA-paclitaxel with $^{111}InCl_3$ in a buffered solution (pH 5.5). Purification was performed by passing the mixture through a C18 Sep-Pak cartridge, yielding ^{111}In-DTPA-paclitaxel with a radiochemical yield of 84%. The purification steps were monitored by HPLC analysis. Eluting the C18 Sep-Pak cartridge with water removed most of the ^{111}In-DTPA (retention time: 2.7 min), which was probably derived from traces of a DTPA contaminant in DTPA-paclitaxel. The radio-chromatogram of ^{111}In-DTPA-paclitaxel (retention time: 12.3 min) correlated with its UV chromatogram, suggesting that the peak at retention time 12.3 min was indeed the target compound (Fig. 2). Under the same chromatographic conditions, paclitaxel had a retention time of 17.1 min. The radiochemical purity of the final preparation was 90% as determined by HPLC analysis.

Stability Studies

7-DTPA-paclitaxel and its indium conjugate displayed considerable stability toward hydrolysis. The estimated half-life based on the disappearance of 7-DTPA-paclitaxel in the phosphate buffered solution (pH 7.4) at 37°C was 30 hr. In rat serum, the half-life was 42 hr, suggesting possible binding of 7-DTPA-paclitaxel with plasma proteins. Conjugation with ^{111}In stabilized 7-DTPA-paclitaxel. As determined by HPLC analysis, 81% and 73% of radioactivity was found still associated with ^{111}In-DTPA-paclitaxel peak after the solution of ^{111}In-DTPA-paclitaxel in saline was allowed to stand at room temperature for 1 day and 7 days, respectively.

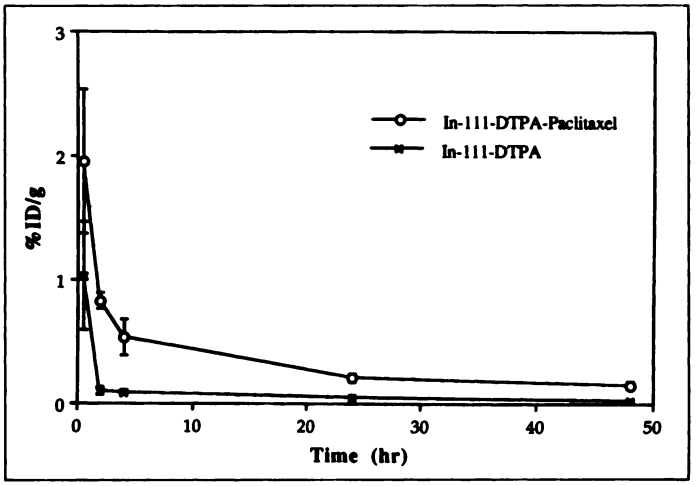

FIGURE 3. Tumor uptake (%ID/g tissue) as a function of time after intravenous administration of ^{111}In-DTPA-paclitaxel or ^{111}In-DTPA in female C3Hf/Kam mice bearing MCA-4 tumors (n = 5, ± s.d.).

In Vitro Cytotoxicity

Cell density-concentration curves were constructed. No significant differences were found for 7-DTPA-paclitaxel and paclitaxel to inhibit cell growth in both cell lines. The minimal concentrations of paclitaxel and DTPA-paclitaxel to inhibit the growth of B16 melanoma cells and 13762 mammary breast cells by 50% (IC_{50}) were determined (Table 1). The results indicated that DTPA-paclitaxel is as effective at inhibiting cell growth as free paclitaxel, suggesting that DTPA-paclitaxel may have a similar mechanism of action as paclitaxel.

In Vivo Biodistribution in Tumor-Bearing Mice

Biodistribution studies were performed in MCA-4 tumor-bearing mice. The mice were injected intravenously with either the ^{111}In-DTPA-paclitaxel or ^{111}In-DTPA. The tissue uptake data of ^{111}In-DTPA-paclitaxel is presented in Table 2 as a percent of the injected dose per gram tissue (%ID/g). A comparison of the tumor uptake for ^{111}In-DTPA-paclitaxel and ^{111}In-DTPA is shown in Figure 3 as %ID/g. Bar graphs of the ratios of tumor-to-blood and tumor-to-muscle are shown in Figure 4.

TABLE 2
Biodistribution of Indium-111-DTPA-Paclitaxel in MCA-4 Mammary Tumor-Bearing Mice*

	30 min	2 hr	4 hr	24 hr	48 hr
Blood	4.36 ± 1.82	1.89 ± 0.49	0.41 ± 0.04	0.003 ± 0.004	0
Lung	5.10 ± 0.70	1.75 ± 0.23	0.53 ± 0.28	0.12 ± 0.02	0.085 ± 0.007
Liver	7.88 ± 1.39	4.70 ± 0.38	3.34 ± 0.76	2.30 ± 0.22	2.00 ± 0.25
Spleen	2.25 ± 0.20	1.43 ± 0.16	0.97 ± 0.27	0.75 ± 0.16	0.61 ± 0.083
Kidney	7.14 ± 1.20	5.01 ± 0.35	4.20 ± 0.82	2.82 ± 0.33	2.25 ± 0.15
Intestine	1.72 ± 0.25	0.85 ± 0.22	2.11 ± 1.06	0.37 ± 0.06	0.32 ± 0.04
Muscle	0.74 ± 0.24	0.25 ± 0.07	0.22 ± 0.14	0.030 ± 0.005	0.027 ± 0.005
Tumor	1.95 ± 0.58	0.82 ± 0.06	0.53 ± 0.14	0.21 ± 0.036	0.15 ± 0.026
Bone	0.95 ± 0.22	0.57 ± 0.18	0.32 ± 0.24	0.046 ± 0.024	0.047 ± 0.015
Heart	2.14 ± 0.36	0.87 ± 0.14	0.28 ± 0.06	0.08 ± 0.012	0.077 ± 0.014
Brain	0.38 ± 0.45	0.066 ± 0.019	0.025 ± 0.011	0	0
Uterus	3.57 ± 1.32	1.18 ± 0.32	0.54 ± 0.13	0.19 ± 0.038	0.19 ± 0.064

*Each mouse received 0.15 ml ^{111}In-DTPA-paclitaxel in saline (5 μCi intravenously). Values at each time point represent the mean ± s.d. of percentage of injected dose per gram of tissue weight (n = 5).

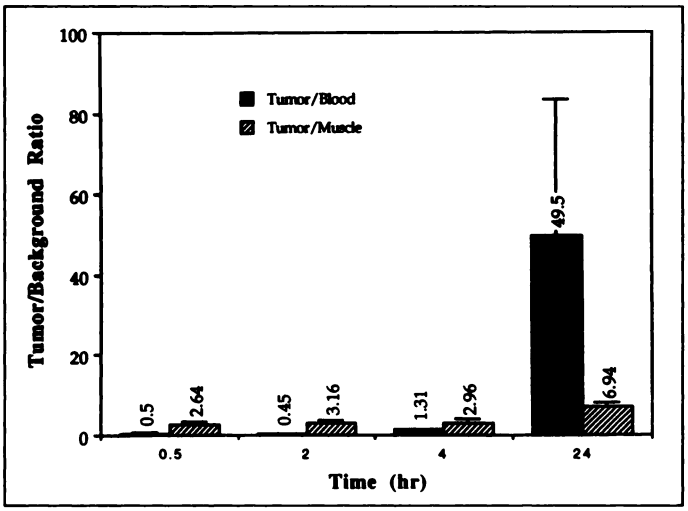

FIGURE 4. Tumor-to-background ratios as a function of time after intravenous administration of ^{111}In-DTPA-paclitaxel in female C3Hf/Kam mice bearing MCA-4 tumors (n = 5, ± s.d.).

The liver and kidney had the greatest tissue-to-plasma ratios at 30 min postinjection, 1.81 and 1.64, respectively. ^{111}In-DTPA-paclitaxel or its metabolites were excreted through both hepatobiliary and urinary routes. The radioactivity in the intestine content reached the maximum at 4 hr, with 15% injected dose found in intestine contents. The peak radioactivity in the urine was reached within 2 hr, being 30% injected dose. Radioactivity in the brain was negligible (Table 2).

The tumor had a substantial uptake of ^{111}In-DTPA-paclitaxel. The tumor uptake of labeled paclitaxel was 8.2-fold greater than that of the ^{111}In-DTPA at 2 hr postinjection, 0.82 and 0.10% ID/g, respectively. Activity (%ID/g) in the tumor of mice injected with ^{111}In-DTPA-paclitaxel was significantly higher than those injected with ^{111}In-DTPA at all time intervals. It was also retained longer in the tumor than was ^{111}In-DTPA (Fig. 3). By 2 hr, 42% of the initial ^{111}In-DTPA-paclitaxel uptake remained in the tumor but only 10% of the ^{111}In-DTPA uptake. A high tumor-to-background ratio is important for radioligands to be useful in tumor imaging. The tumor-to-muscle ratio increased from 2.64 at 30 min to 6.94 at 24 hr. The tumor-to-blood ratio was larger than 1 at 4 hr and reached 50 at 24 hr after injection (Fig. 4). The tumor-to-blood ratio at 48 hr was not listed because the extremely low blood activity caused large variation.

Imaging Studies

Tumors were clearly visualized in animals injected with ^{111}In-DTPA-paclitaxel in gamma scintigraphy images at all time intervals observed. Images obtained at 2 hr and 24 hr after injection are presented in Figure 5A and B. For comparison, images obtained with ^{111}In-DTPA are presented in Figure 5C and D. As expected, ^{111}In-DTPA was characterized by rapid clearance from the plasma and high excretion in the urine with negligible retention in the tumor. Other major organs or body parts, such as the liver, kidney and intestine, had minimal retention of ^{111}In-DTPA. At 24 hr, most radioactivity was cleared from the body.

Autoradiography

Autoradiography was used to evaluate the local distribution of ^{111}In-DTPA-paclitaxel in the tumor. At 2 hr postinjection, tumor uptake of the radiotracer was clearly visualized (Fig. 6).

DISCUSSION

Our interest in indium-labeled paclitaxel was prompted by its potential as a tumor localization agent and the possibility that it might be useful to predict the response of Taxol therapy and thus select proper patients for expensive treatment. The possible use of radiolabeled chemotherapeutic agents as an imaging tool for the prediction of drug efficacy has been proposed using ^{18}F-5-fluorouracil as a model compound (*6,7*). Later studies in nude mice bearing a 5-FU-sensitive or a 5-FU-resistant tumor have found that the efflux of the ^{18}F activity from the tumor was correlated with the 5-FU sensitivity of the tumor (*8*), suggesting potential use of radiolabeled 5-FU as a prognostic agent. We have synthesized ^{111}In-labeled paclitaxel using DTPA as a chelating agent. Paclitaxel has two hydroxyl groups that can be most conveniently functionalized: 2′-hydroxyl and 7-hydroxyl groups. Previous studies on the structure-property relationship of paclitaxel analogs have showed that 7-substituted paclitaxel derivatives maintain their ability to promote microtubule assembly and do not appear to be critical to receptor binding (*9*). Furthermore, C-7 esters have been shown to be more stable than C-2′ derivatives (*10*). Therefore, our efforts were focused on the preparation of 7-DTPA-paclitaxel. When paclitaxel was reacted with DTPA anhydride, both 2′- and 7-paclitaxel DTPA ester were obtained. Aqueous treatment followed by preparative

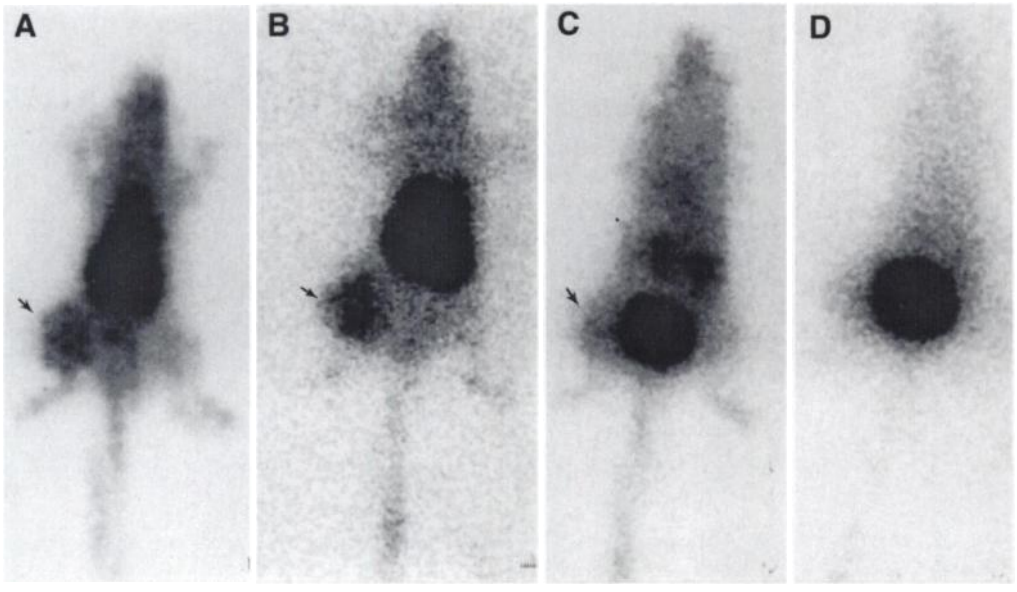

FIGURE 5. Planar, static whole-body gamma scintigrams in C3Hf/Kam mice bearing MCA-4 tumors. The mice were imaged after intravenous injection of ^{111}In-DTPA-paclitaxel (A = 1 hr; B = 24 hr) or ^{111}In-DTPA (C = 30 min; D = 2 hr). Arrow indicates tumor. For mice injected with ^{111}In-DTPA-paclitaxel, activity is retained in the tumor.

FIGURE 6. Autoradiogram taken of sectioned mouse (100 μm) injected with ^{111}In-DTPA-paclitaxel and killed 2 hr later. Arrow indicates tumor.

reversed-phase TLC gave 7-DTPA-paclitaxel in 10% overall yield. The 7-DTPA-paclitaxel displayed reasonable stability both before and after conjugation with ^{111}In.

Substitution with DTPA at the C-7 position did not cause significant change in cytotoxicity. The 7-DTPA-paclitaxel inhibited cell growth of both cell lines tested (B16 mouse melanoma cells and 13762 mammary breast cells) to the similar extent as free paclitaxel. It is interesting to note that other 7-substituted paclitaxel derivatives also display similar activity as free paclitaxel (*9,10*). It may be reasonable to assume that the mechanism of action of 7-DTPA-paclitaxel may resemble that of paclitaxel. In fact, ^{111}In-DTPA-paclitaxel exhibited a pharmacological profile resembling that of paclitaxel (*11*). Radioactivity in the brain was negligible. The liver had the greatest tissue-to-plasma ratios. Hepatobiliary excretion of radiolabeled DTPA-paclitaxel or its metabolites was one of the major routes for the clearance of the drug from the blood, as evidenced by the presence of a large amount of radioactivity in the intestine contents 4 hr after injection. However, due to the hydrophilic nature of DTPA-paclitaxel, a significant amount of ^{111}In-DTPA-paclitaxel or its degradation products was also excreted through the kidney, which only played a minor role in the clearance of paclitaxel.

The synthesis of indium-labeled paclitaxel is the first attempt to use paclitaxel for nuclear imaging purposes. Indium-111-DTPA-paclitaxel had a substantial initial uptake in the tumor and was retained for a prolonged period in our mice/MCA-4 mammary tumor model. Since the ^{111}In-DTPA control was quickly cleared from the blood and from other body parts, the observed data should represent the behaviors of radiolabeled paclitaxel, rather than that of ^{111}In-DTPA possibly produced by degradation of ^{111}In-DTPA-paclitaxel. In gamma scintigraphic studies, the tumor was clearly visualized in mice injected with ^{111}In-DTPA-paclitaxel but not in mice injected with ^{111}In-DTPA. Selective uptake of ^{111}In-DTPA-paclitaxel in the tumor also was evidenced by autoradiographic studies. With insignificant blood-pool activity and moderate tumor uptake, ^{111}In-DTPA-paclitaxel may be a useful radiotracer for tumor imaging. Because of hepatobiliary clearance and significant intestinal activity, imaging tumors in the abdominal area with ^{111}In-DTPA-paclitaxel could be potentially troublesome.

It is not clear with the existing data whether the retention of ^{111}In-DTPA-paclitaxel in the tumor is due to biding to neoformed blood vessels or due to intracytoplasmic biding to the cytoskeleton or microtubules. Neither is it clear whether the patchy ^{111}In-DTPA-paclitaxel distribution within tumors observed in autoradiography reflect blood flow supply to the lesions or some more specific binding of the drug to well-defined constituents of the tumor. Studies aimed at assessing whether a correlation exists between the tumor uptake of ^{111}In-DTPA-paclitaxel and the antitumor efficacy of 7-DTPA-paclitaxel are underway in our laboratory.

CONCLUSION

We have conjugated DTPA to paclitaxel. The resulting compound, 7-DTPA-paclitaxel, had cytotoxicity similar to that of free paclitaxel. Indium-labeled DTPA-paclitaxel demonstrated a high tumor uptake and prolonged retention in the tumor in mice bearing MCA-4 mammary tumor. Gamma scintigraphy and autoradiographic studies confirmed the retention of radiolabeled paclitaxel in the tumor. This agent may be a useful ligand for tumor localization and for the studies of the action of paclitaxel.

ACKNOWLEDGMENTS

This work was supported by the George and Cleo Cook Fund. We thank Li-Ren Kuang, Migual Diaz and Valentine Boving for their expert technical support.

REFERENCES

1. Horwitz SB, Cohen D, Rao S, Ringel I, Shen H-J, Yang, C-P. Taxol, mechanisms of action and resistance. *J Natl Cancer Inst Monographs* 1993;15:55–61.
2. Holmes FA, Kudelka AP, Kavanag JJ, Huber MH, Ajani JA, Valero V. Current status of clinical trials with paclitaxel and docetaxel. In: Georg GI, Chen TT, Ojima I, Vyas DM, eds. *Taxane anticancer agents: basic science and current status.* Washington, DC: American Chemical Society; 1995:31–57.
3. Marie A, Okaba C, Hunter WL, Arsenault AL. Taxol: a potent inhibitor of normal and tumor-induced angiogenesis. *Proceedings of the American Association for Cancer Research* 1995;36:454.
4. Beijnen JH, Huizing MT, ten Bokkel Huinink WW, et al. Bioanalysis, pharmacokinetics and pharmacodynamics of the novel anticancer drug paclitaxel. *Semin Oncol* 1994;21:53–62.
5. Milas L, Hunter NR, Mason KA, Kurdoglu B, Peters LJ. Enhancement of tumor radioresponse of a murine mammary carcinoma by paclitaxel. *Cancer Res* 1994;54: 3506–3510.
6. Shani J, Wolf W, Schlesinger T, et al. Distribution of ^{18}F-5-fluorouracil in tumor-bearing mice and rats. *Int J Nucl Med Biol* 1978;5:19–28.
7. Fowler JS, Finn RD, Lambrecht RM, Wolf AP. The synthesis of ^{18}F-5-fluorouracil. *J Nucl Med* 1972;14:63–64.
8. Visser GWM, Gorree GCM, Braakhuis BJM, Herscheid JDM. An optimized synthesis of ^{18}F-labeled 5-fluorouracil and a reevaluation of its use as prognostic agent. *Eur J Nucl Med* 1989;15:225–229.
9. Suffness M. Overview of paclitaxel research. In: Georg GI, Chen TT, Ojima I, Vyas DM, eds. *Taxane anticancer agents: basic science and current status.* Washington, DC: American Chemical Society; 1995:1–17.
10. Mathew AE, Mejillano MR, Nath JP, Himes RH, Stella VJ. Synthesis and evaluation of some water-soluble prodrugs and derivatives of taxol with antitumor activity. *J Med Chem* 1992;35:145–151.
11. Eiseman JL, Eddington N, Leslie J, et al. Plasma pharmacokinetics and tissue distribution of paclitaxel in CD2F1 mice. *Cancer Chemother Pharmacol* 1994;34:465–471.